American Mineralogist, Volume 71, pages 746–757, 1986

Role of Na in the structure of low-cordierite: A single-crystal X-ray study

THOMAS ARMBRUSTER
Laboratorium für chemische und mineralogische Kristallographie, Universität Bern, Freiestrasse 3, CH-3012 Bern, Schweiz

ABSTRACT

Crystal structures of four natural Na-rich cordierites (space group *Cccm*) refined at room temperature are described. Electron-microprobe, Li and Be analyses, and structure refinements indicate the substitutions $Na^+ + Be^{2+} \rightarrow Al^{3+}$ and $Na^+ + Li^+ \rightarrow Mg^{2+}$ or Fe^{2+}. All crystals exhibit a high degree of (Si,Al) ordering typical of low-cordierites. The effect of Na on the structure is determined by comparison with previously reported structures of Na-poor crystals. Partial incorporation of Na in the center of the six-membered ring of oxygen atoms ($O_2$3-$O_2$6-$O_2$1-$O_2$3-$O_2$6-$O_2$1) causes the rings to predominantly compress along the **b**-axis, whereas the larger six-membered rings of cations ($T_2$3-$T_2$6-$T_2$1-$T_2$3-$T_2$6-$T_2$1) slightly expand along the same direction. These opposing motions lead to an increase in the **b**-axis and are responsible for a nearly hexagonal lattice geometry in Na-rich cordierites. Linear regression analyses reveal that tetrahedral angles (O–T–O) and individual T–O bonds are affected by Na content. The Al tetrahedron $T_1$1, interconnecting six-membered rings of tetrahedra, is the preferred site for Be substitution in cordierite. The smaller ionic radius of Be significantly decreases the mean $T_1$1–O bond length. Li partially occupies octahedral positions and substitutes for Mg or Fe. All Na-rich cordierites studied are also H_2O rich because each Na attracts two water molecules into the adjacent structural cavities to complete its coordination polyhedron of eight oxygen atoms.

INTRODUCTION

Cordierites are silicates with a tetrahedral framework structure and the simplified formula $(Mg,Fe)_2Al_4Si_5O_{18}$. Based on the assignment of Cohen et al. (1977), a crystal chemical formula of low-cordierite (space group *Cccm*) can be written as follows:

$$(M)_2(T_2 3)_2(T_2 1)_2(T_2 6)_2(T_1 6)(T_1 1)_2O_{18},\ (Ch0,Ch¼)$$

where M represents an octahedrally coordinated metal ion (e.g., Mg^{2+}, Fe^{2+}, or Mn^{2+}) and T represents a tetrahedral position (Fig. 1). In particular, T_2 tetrahedra build six-membered rings, and T_1 tetrahedra cross-link these units to form a framework. $T_1$1 and $T_2$6 are occupied by Al whereas all other tetrahedra are occupied by Si. This preferred (Si,Al) distribution gives rise to orthorhombic symmetry, in contrast to the disordered arrangement in hexagonal high-cordierites (space group *P6/mcc*). The six-membered rings produce endless channels parallel to **c**. The channel position at 0,0,0 in the center of the six-membered ring is designated Ch0. The position at 0,0,¼, in the middle of a larger cavity situated between two six-membered rings, is designated Ch¼. Charge deficiency in the framework structure can be balanced by incorporation of additional atoms in either channel position. A more detailed description of the structure is given in Gibbs (1966), Cohen et al. (1977), Hochella et al. (1979), and Wallace and Wenk (1980).

This study was mainly performed to explain how Na in the structure of cordierite induces lattice distortions and to use crystal-structure refinements as an analytical tool to understand the substitution mechanisms that allow Na to be incorporated.

Natural cordierites often contain substantial amounts of Na_2O. The concentration of Na_2O cannot be determined by wet chemical analyses because they may give erratic results owing to sheet-silicate inclusions (pinite) in cordierite. However, the microprobe analyses of Lepezin et al. (1974) indicate Na_2O concentrations up to 1.4 wt%. The most Na-rich cordierite (6 wt% Na_2O) was reported by Fuchs (1969) from the Allende meteorite. Several authors gave considerable attention to Na-rich cordierites and studied the influence of Na on cordierite crystal chemistry and properties (Černý and Povondra, 1966; Newton, 1966; Povondra and Langer, 1971; Povondra and Čech, 1978; Schreyer et al., 1979; Selkregg and Bloss, 1980; Armbruster and Irouschek, 1983; Povondra et al. (1984). The crystal structure of a Na-rich cordierite from Haddam, Connecticut, was first refined by Meagher (1967), who could not decide whether Na is situated on Ch0 or Ch¼. In the structural refinement of a Fe-rich cordierite from Dolni Bory (Czechoslovakia) with 0.15 Na per formula (based on 18 oxygens), Hochella et al. (1979) assigned Na to the Ch0 position. When a natural Na- and H_2O-rich crystal was degassed (Armbruster, 1985a), the subsequent single-crystal structure refinement proved that

0003–004X/86/0506–0746$02.00

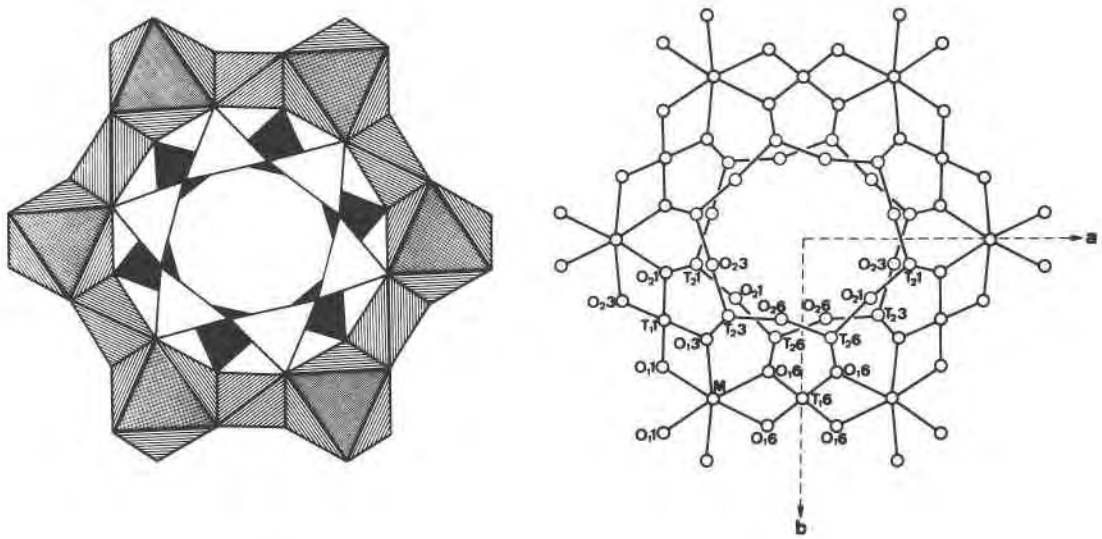

Fig. 1. Characteristic portion of the low-cordierite structure viewed parallel to the **c** axis. The nomenclature of atomic positions is adopted from Cohen et al. (1977). The endless structural channels, running parallel to the **c** axis, may host water molecules at the height $z = ¼$ (Ch¼) and Na at the height $z = 0$ (Ch0). $T_1$1 and $T_2$6 are occupied by Al, whereas $T_1$6, $T_2$3, and $T_2$1 are occupied by Si. The M site is octahedrally coordinated by oxygen and is occupied by Mg, Fe, Mn, and Li.

the Ch¼ position became empty while a strong difference-Fourier peak remained at Ch0, which supports the assignment of Na to Ch0 and H_2O to Ch¼. Goldman et al. (1977) suggested on the basis of IR single-crystal experiments that metal ions (Na^+, Ca^{2+}, or Fe^{2+}) in Ch0 cause a special water orientation at Ch¼. This is designated "type II water," where the plane of the water molecule lies in (100) with the H-H vector parallel to the **b**-axis. For "type I water," characteristically found in Na-poor samples, the plane of the molecule also lies in (100) but the H-H vector is parallel to **c**. On the basis of NMR results, Carson et al. (1982) reinterpreted type I as a molecule in rapid motion between the orientations with H-H parallel to **c** and H-H perpendicular to **c**.

Sample description

All cordierites used in this structural investigation have already been described by various authors who kindly supplied fragments of their material. Chemical analyses were also adopted from previous papers. Even precise electron-microprobe analyses on the same grain on which the structure study is performed are not unambiguous if light elements such as Li and Be are present. Calculation of these elements by difference is hampered because the nature of the substitution reaction is often unknown and the variable Fe^{2+}/Fe^{3+} ratio introduces an additional degree of freedom.

The Na- and Be-bearing cordierite labeled "Sponda" originates from Alpe Sponda, Central Alps, Switzerland (Armbruster and Irouschek, 1983). The composition of the Sponda crystals shows significant differences in the degree of $Na^+ + Be^{2+} \rightarrow Al^{3+}$ substitution: $Na_{0.23-0.32}Li_{0.02-0.04}Mg_{1.40-1.49}Fe_{0.50-0.60}Mn_{0.01-0.02}Al_{3.76-3.91}$-$Be_{0.15-0.21}Si_{4.94-4.97}O_{18}$. About 60% of the structural cavities are occupied by water, and CO_2 is only a minor constituent. Refractive index measurements using the double variation method with the spindle stage (Bloss, 1981) yielded for one particular crystal $n_\alpha = 1.5495$, $n_\beta = 1.5559$, and $n_\gamma = 1.5581$. $2V_X = 57.3°$ was calculated from extinction measurements at 589.3 nm. The relatively low refractive indices and the high optic angle compared to other crystals from this locality suggest that the studied crystal contains relatively little Na and Be (Armbruster and Irouschek, 1983). The cell dimensions (Table 1) are very similar to those of sample "Sponda 99" (Armbruster and Irouschek, 1983). Therefore, the chemical formula for Sponda 99 was used for the structure refinement of Sponda (Table 2).

The sodian-beryllian cordierite "Kemiö" comes from Gammelmorskärr (Kemiö Island, Finland). Povondra et al. (1984) did a detailed study of this cordierite and its decomposition products. Cell dimensions of the Kemiö crystal (Table 1) are within 1σ of those obtained from powder data (Povondra et al., 1984).

Ferry (1980) studied a pelitic schist from south-central Maine where he found the assemblage garnet-cordierite-sillimanite-quartz (his A666). In thin sections the cordierite is very fine grained and often shows undulatory extinction or complicated twinning and

Table 1. Cell dimensions [Å] and details of data collection

crystal	Sponda	Kemiö	Ferry	Haddam
number of observations	1196	1187	1198	2528
number of contributions*	1140	1102	1133	2367
R - Rw [%]	2.0-3.2	2.1-3.5	1.9-2.7	2.0-2.7
extinction**	6.7	9.1	0.7	2.7
a	17.060(2)	17.065(2)	17.056(3)	17.054(1)
b	9.759(1)	9.797(2)	9.783(2)	9.759(2)
c	9.322(2)	9.293(2)	9.335(2)	9.324(1)
V [Å^3]	1552.0	1553.7	1557.6	1551.8
Δ***	0.172	0.105	0.122	0.165

* reflections for which F(obs) < 6σ F(obs) with F(calc) < F(obs) were rejected

** isotropic extinction coefficient (· 10^3)

*** $\Delta = 1.094 \cdot (a-b \cdot \sqrt{3})$

Table 2. Atomic populations of mixed or partially occupied sites

crystal	M	$T_1$1	ChO	Ch1/4
Sponda	Mg: 0.7 Fe: 0.3	Al: 0.92 Be: 0.08	Na: 0.25	O: 0.6
Kemiö	Mg: 0.38 Fe: 0.55 Li: 0.07	Al: 0.80 Be: 0.20	Na: 0.47*	O: 0.8*
Ferry	Mg: 0.53 Fe: 0.29 Li: 0.18	Al: 1.00	Na: 0.36	O: 0.85
Haddam	Mg: 0.66 Fe: 0.29 Li: 0.05	Al: 0.92 Be: 0.08	Na: 0.27	O: 0.75

* refined occupancy

intergrowth. Striking are strong pleochroic haloes around solid inclusions (zircons). The haloes turn yellow orange with the polarizer parallel to the **c**-axis, but are colorless with the polarizer parallel to **a** or **b**. The specimen studied (designated "Ferry" in Table 2) has $2V_X = 55.8°$ with $n_\alpha = 1.5556$, n_β(calc.) = 1.5634, and $n_\gamma = 1.5656$. Even though a Be analysis is not available for this sample, the stoichiometric ratio Si/Al = ¾ suggests that this specimen is Be-free. The deficit in the sum of octahedrally coordinated cations (Mg + Fe + Mn) determined by electron microprobe is 1.64 versus 2.0 for stoichiometric cordierites.

The most-studied Na- and Be-bearing cordierites come from the locality Haddam, Connecticut (Newton, 1966; Povondra and Čech, 1978). Crystal-structure refinements were carried out by Meagher (1967) and Armbruster (1985a). Precise optical data and cell dimensions were collected by Selkregg and Bloss (1980). Single-crystal IR spectra interpreted by Goldman et al. (1977) show 82% water of type II and 18% water of type I. Heating experiments at 1000°C in a buffered atmosphere (Armbruster, 1985a) removed the electron density at Ch¼. The optical properties of the Haddam crystal agree with those determined by Selkregg and Bloss (1980). Coulometric analyses of the volatile channel occupants lead to 2.3 wt% H_2O and 0.12 wt% CO_2 (Armbruster and Irouschek, 1983), which amounts to 75% occupation of the Ch¼ position.

Experimental method

Crystals used for each structure refinement were of quite regular shape with dimensions between 150 and 300 μm. Absorption was considered to be negligible. Great care was taken to pick inclusion-free specimens that revealed sharp extinction between crossed nicols at all spindle positions of a spindle-stage-equipped microscope (Bloss, 1981). Cell dimensions of the crystals Sponda, Kemiö, and Ferry were refined from the scattering vectors of 22 reflections (*hkl*: 0,12,0; 16,0,0; 008; 12,4,6; 9,11,7; and their symmetric equivalents) using graphite-monochromated Mo$K\alpha$-radiation. For the Haddam specimen, the reflections with *hkl* values of 22,4,6; 9,11,7; 0,12,0; 0,0,16; 16,0,0; and their symmetric equivalents were used for cell refinement. All X-ray measurements were performed on an Enraf Nonius CAD4 single-crystal diffractometer. Reflection intensities allowing for *C*-centering were collected in one quadrant of reciprocal space employing an ω-mode to $\theta = 30°$ (Mo$K\alpha$). For the Haddam crystal, intensities up to $\theta = 40°$ were measured. Reflections for which $\sigma(I)/I > 0.5$ were flagged as weak. The final scan speed was calculated from a prescan in order to obtain $\sigma(I)/I = 0.03$. Intensity of standard reflections measured after each hour of X-ray exposure agreed within 3% for all crystals. Four orientation-control reflections were monitored every 100 reflections. Data reduction, including background and Lorentz-polarization corrections, was achieved using the SDP program system (Enraf Nonius, 1983). Structure factors of the type 0*kl* and *h*0*l*, where *l* is odd (*c*-glide), were rejected (Table 1). *The X-ray System of Crystallographic Programs* (Stewart et al., 1976) was used for all structural refinements.

Reflections were weighted on the basis of counting statistics, and those with $F_{obs} < 6\sigma F_{obs}$, where $F_{calc} < F_{obs}$, were excluded from the refinement. Starting coordinates for all refinements were taken from the Haddam cordierite of Meagher (1967), and neutral atom scattering factors supplied with the program were used. Real and imaginary parts of the anomalous dispersion corrections were also included for all atoms. Analyses reported in the literature were taken to calculate the Fe/Mg ratio in the M site. Be in the Sponda, Kemiö, and Haddam specimens was assigned to $T_1$1 following Meagher (1967). Analytically determined Na was assigned to Ch0 and water, as estimated from optical properties (Armbruster and Irouschek, 1983) or from chemical analyses, to Ch¼. The differences between observed and calculated structure factors in these initial refinements with anisotropic temperature factors indicated that a correction for secondary extinction had to be made. In addition, temperature factors for the M position seemed too high for some crystals compared to other cordierites previously studied in our laboratory. The scattering power attributed to this site was obviously too strong, and it had to be assumed that a light element had been neglected or the Mg concentration in M was underestimated. For the Haddam cordierite, a significant Li concentration had been previously determined (Armbruster and Irouschek, 1983). In the Ferry and the Kemiö crystals for which Li analyses were not available, the sum of cations assigned to the octahedrally coordinated position (Mg,Fe,Mn) was considerably less than the ideal value of 2. For the Ferry crystal, which had the largest deviation from 2, the structure refinement resulted in the highest temperature factors on M. If the mean M–O distances are plotted against the prescribed *F*-value [F_{mol} = Fe/(Mg + Fe + Mn)], the points are in fair agreement with the results of Wallace and Wenk (1980) (their Fig. 3). These observations lead to the conclusion that the unaccounted element at M must have an ionic radius (Shannon, 1976) between Mg^{2+} (0.72 Å) and F^{2+} (0.78Å), which is fulfilled by Li^+ (0.76 Å). The Li occupation on M was calculated as $Li^+ = 1 - [n(Fe^{2+}) + n(Mn^{2+}) + n(Mg^{2+})]/2$, where n stands for the number of atoms calculated on the basis of 18 oxygen atoms. After completion of the structural studies, an atomic absorption Li_2O analysis (G. Werding, Bochum) on a cordierite concentrate of the A666 specimen (Ferry, 1980) disclosed 0.53 wt% Li_2O, that is, 0.22 Li per formula unit. As judged from the Na content and the temperature factor of the M site, the single crystal used for the structure refinement exhibited even much higher Li concentrations (Table 2). Another problem occurred in the Kemiö refinement. The temperature factors at Ch0 and Ch¼ became negative indicating a higher occupation at these sites than suggested by the Na content and optical data taken from the literature. A site occupation refinement of Na at the Ch0 site and of O at Ch¼ increased the occupation of Na from 0.39 to 0.47 and that of water from 0.5 to 0.8. The resulting vibrational parameters increased to similar values as observed for the other crystals. The final refinements, including correction for secondary extinction and allowing for Li in M, yielded extinction parameters and *R*

Table 4. Fractional coordinates and temperature factors U_{ij} ($\times 10^2$), estimated standard deviations in parentheses

	Sponda	Kemiö	Ferry	Haddam
O_1^1				
x^1	0.24614(6)	0.24458(7)	0.24549(7)	0.24592(4)
y	-0.10433(11)	-0.10606(12)	-0.10446(12)	-0.10438(8)
z	0.35857(11)	0.35763(15)	0.35842(14)	0.35850(8)
U_{11}	1.18(5)	1.35(6)	1.21(5)	1.20(3)
U^{11}	0.86(4)	0.95(6)	0.83(6)	0.80(3)
U^{22}	0.94(5)	1.06(6)	0.73(6)	0.83(3)
U^{33}	-0.05(4)	0.01(5)	-0.06(4)	-0.04(2)
U^{12}	0.29(4)	0.41(5)	0.29(4)	0.35(2)
U^{13}	-0.09(4)	-0.01(5)	-0.06(4)	-0.07(2)
B^{23}_{eq}	0.78	0.88	0.73	0.74
O_1^6				
x^1	0.06196(6)	0.06148(7)	0.06140(7)	0.06187(4)
y	-0.41577(11)	-0.41548(12)	-0.41540(12)	-0.41574(7)
z	0.34876(12)	0.34870(14)	0.34868(13)	0.34885(8)
U_{11}	0.74(5)	0.96(6)	0.78(5)	0.83(3)
U^{11}	1.13(5)	1.15(6)	1.20(5)	1.02(3)
U^{22}	0.94(5)	0.96(6)	0.81(6)	0.81(3)
U^{33}	-0.08(4)	-0.13(4)	-0.19(4)	-0.14(2)
U^{12}	0.00(4)	0.10(5)	0.02(5)	0.03(2)
U^{13}	-0.33(4)	-0.34(4)	-0.36(5)	-0.32(2)
B^{23}_{eq}	0.74	0.81	0.73	0.70
O_1^3				
x^1	-0.17344(6)	-0.17377(8)	-0.17273(7)	-0.17331(4)
y	-0.30866(10)	-0.30681(13)	-0.30701(12)	-0.30849(7)
z	0.35804(12)	0.35715(15)	0.35842(13)	0.35792(9)
U_{11}	1.00(5)	1.16(6)	0.96(5)	0.94(3)
U^{11}	1.05(5)	1.18(7)	1.07(6)	1.02(3)
U^{22}	0.95(5)	1.02(7)	0.71(7)	0.86(3)
U^{33}	0.16(4)	0.11(5)	0.25(4)	0.11(2)
U^{12}	-0.11(4)	-0.17(5)	-0.18(4)	-0.17(2)
U^{13}	-0.26(4)	-0.35(5)	-0.19(5)	-0.28(3)
B^{23}_{eq}	0.79	0.88	0.72	0.74
O_2^6				
x^2	0.04328(9)	0.04344(11)	0.04256(10)	0.04315(6)
y	-0.24612(16)	-0.24302(20)	-0.24250(19)	-0.24496(12)
z	0	0	0	0
U_{11}	0.59(7)	0.66(9)	0.59(8)	0.62(4)
U^{11}	1.63(7)	1.67(9)	1.61(9)	1.43(5)
U^{22}	1.96(8)	2.03(11)	1.89(10)	1.90(6)
U^{33}	-0.21(6)	-0.17(7)	-0.13(6)	-0.16(3)
U^{12}	1.10	1.15	1.08	1.04
B^{12}_{eq}				
O_2^1				
x^2	0.12039(10)	0.11723(12)	0.11916(11)	0.11975(7)
y	0.18225(16)	0.17903(20)	0.18157(18)	0.18176(11)
z	0	0	0	0
U_{11}	1.19(8)	1.24(9)	1.38(9)	1.21(5)
U^{11}	1.27(8)	1.28(10)	1.21(9)	1.14(5)
U^{22}	1.87(8)	2.14(11)	1.79(10)	1.81(6)
U^{33}	0.58(6)	0.57(7)	0.65(7)	0.61(4)
U^{12}	1.14	1.23	1.15	1.09
B^{12}_{eq}				
O_2^3				
x^2	0.16356(9)	0.16260(11)	0.16287(10)	0.16350(7)
y	-0.07844(15)	-0.07703(19)	-0.07747(17)	-0.07847(11)
z	0	0	0	0
U_{11}	1.36(8)	1.50(10)	1.47(9)	1.44(5)
U^{11}	0.65(7)	0.70(9)	0.75(8)	0.59(4)
U^{22}	1.92(8)	2.21(11)	1.88(10)	1.85(6)
U^{33}	-0.31(6)	-0.35(7)	-0.37(7)	-0.35(4)
U^{12}	1.03	1.16	1.08	1.02
B^{12}_{eq}				
T_1^1 (Al,Be)				
x^1	1/4	1/4	1/4	1/4
y	1/4	1/4	1/4	1/4
z	0.25010(10)	0.25007(11)	0.25018(9)	0.25011(6)
U_{11}	0.83(3)	0.80(4)	0.87(3)	0.76(2)
U^{11}	0.68(3)	0.70(4)	0.78(3)	0.61(2)
U^{22}	0.78(3)	0.77(5)	0.53(3)	0.61(2)
U^{33}	0.12(2)	0.10(3)	0.07(2)	0.10(1)
U^{12}	0.60	0.60	0.57	0.52
B^{12}_{eq}				

	Sponda	Kemiö	Ferry	Haddam
T_1^6 (Si)				
x^1	0	0	0	0
y	1/2	1/2	1/2	1/2
z	1/4	1/4	1/4	1/4
U_{11}	0.63(4)	0.68(4)	0.66(4)	0.60(2)
U^{11}	0.72(4)	0.75(4)	0.73(4)	0.66(2)
U^{22}	0.62(4)	0.67(4)	0.47(5)	0.48(2)
B^{33}_{eq}	0.52	0.55	0.49	0.45
T_1^1 (Si)				
x^2	0.19177(3)	0.19092(4)	0.19140(4)	0.19179(2)
y	0.07870(6)	0.07963(7)	0.07894(6)	0.07870(4)
z	0	0	0	0
U_{11}	0.62(3)	0.63(3)	0.54(3)	0.55(1)
U^{11}	0.50(3)	0.58(3)	0.48(3)	0.45(1)
U^{22}	0.74(3)	0.87(3)	0.56(3)	0.61(2)
U^{33}	0.02(2)	0.03(2)	0.03(2)	0.02(1)
B^{12}_{eq}	0.49	0.55	0.42	0.42
T_2^3 (Si)				
x^2	-0.13562(3)	-0.13639(4)	-0.13524(4)	-0.13563(2)
y	0.23649(6)	0.23546(7)	0.23542(6)	0.23636(4)
z	0	0	0	0
U_{11}	0.56(3)	0.60(3)	0.49(3)	0.51(1)
U^{11}	0.58(3)	0.63(3)	0.57(3)	0.52(1)
U^{22}	0.76(3)	0.91(3)	0.54(3)	0.63(2)
U^{33}	-0.05(2)	-0.06(2)	-0.11(3)	-0.06(1)
B^{12}_{eq}	0.50	0.56	0.42	0.44
T_2^6 (Al)				
x^2	0.05051(4)	0.04994(4)	0.05052(4)	0.05052(3)
y	0.30825(6)	0.30859(7)	0.30935(7)	0.30856(4)
z	0	0	0	0
U_{11}	0.58(3)	0.59(3)	0.48(3)	0.51(2)
U^{11}	0.62(3)	0.64(4)	0.63(3)	0.58(2)
U^{22}	0.68(3)	0.77(4)	0.55(3)	0.57(2)
U^{33}	0.05(2)	0.08(2)	0.06(2)	0.06(1)
B^{12}_{eq}	0.49	0.53	0.44	0.44
M (Mg,Fe,Mn,Li)				
x	0.33632(6)	0.33488(11)	0.33680(9)	0.33622(6)
y	0	0	0	0
z	1/4	1/4	1/4	1/4
U_{11}	0.86(6)	0.57(13)	0.59(7)	0.67(3)
U^{11}	1.12(6)	1.25(13)	0.69(7)	0.93(3)
U^{22}	1.12(6)	0.91(12)	0.87(7)	0.85(3)
U^{33}	0.02(4)	0.01(8)	0.02(6)	0.00(3)
B^{23}_{eq}	0.82	0.72	0.57	0.64
ChO (Na)				
x	0	0	0	0
y	0	0	0	0
z	0	0	0	0
U_{11}	3.3(4)	2.8(2)	2.4(3)	2.4(2)
U^{11}	2.2(3)	2.0(2)	1.6(3)	1.1(2)
U^{22}	4.9(5)	4.7(3)	4.1(4)	4.1(3)
U^{33}	0.3(3)	0.0(3)	0.2(2)	0.1(2)
U^{12}	2.7	2.5	2.1	2.0
B_{eq}				
Chl/4 (O)				
x	0	0	0	0
y	0	0	0	0
z	1/4	1/4	1/4	1/4
U_{11}	10.9(7)	8.8(5)	12.3(6)	12.8(5)
U^{11}	5.4(4)	5.0(3)	5.9(4)	6.6(3)
U^{22}	5.4(5)	3.3(3)	3.5(3)	4.9(3)
B^{33}_{eq}	5.7	4.5	5.7	6.4

values as listed in Table 1. Difference-Fourier maps around framework atoms did not disclose residual densities greater than ± 0.3 e/Å^3. Residual peaks in the structural channels are discussed in the corresponding section. Final observed and calculated structure factors for all data sets are listed in Table 3.[1] Fractional coordinates are given in Table 4.

Results and interpretation

Interatomic distances and angles

A striking variation in bond lengths is observed within the tetrahedron $T_1$1, whose central position is partially occupied by Al and Be. It had previously been shown (Armbruster, 1985b) that this polyhedron slightly decreases in size with increasing ionic radius of the atom in the M site, i.e., for (Mg,Fe)-cordierites with increasing Fe content. Thus the mean $T_1$1–O distances were corrected for this effect. Figure 2, which also includes the presumably Be-free cordierites of Wallace and Wenk (1980), displays the correlation between Be substitution and corrected mean $T_1$1–O bond lengths. In beryl (Gibbs et al., 1968; Morosin, 1972) where Be occupies a similar position interconnecting Si_6O_{18} rings, the Be–O distance varies between 1.653 and 1.666 Å, whereas in Be-free Mg-cordierites, the corresponding $T_1$1(Al)–O bond length is about 1.756 Å. A solid line in Figure 2, agreeing well with the observed Be → Al substitution, is drawn to elucidate this relationship. The assumption that the tetrahedron $T_1$1 of

[1] To obtain a copy of Table 3, order Document AM-86-302 from the Business Office, Mineralogical Society of America, 1625 I Street, N.W., Suite 414, Washington, D.C. 20006. Please remit $5.00 in advance for the microfiche.

Table 5. Selected interatomic distances (Å) and O–T–O, T–O–M, and T–O–T angles [estimated standard deviations (in parentheses) of the Ferry cordierite also refer to the Sponda and Kemiö data]

dist./angl.	mult.	Sponda	Kemiö	Ferry	Haddam
$T_1 1$-$O_1 1$	(2)	1.747	1.729	1.750(1)	1.746(1)
-$O_1 3'$	(2)	1.745	1.731	1.752(1)	1.746(1)
Mean		1.7460	1.7300	1.7510	1.7460
$O_1 3''$-$T_1 1$-$O_1 3'$	(1)	109.59	109.62	109.55(5)	109.67(3)
$O_1 1$-$T_1 1$-$O_1 3''$	(2)	95.49	96.47	96.21(5)	95.61(4)
$O_1 3'$	(2)	124.97	123.70	124.07(5)	124.77(4)
-$O_1 1'$	(1)	109.11	109.22	109.18(5)	109.12(4)
Mean		109.94	109.86	109.86	109.93
$T_1 6$-$O_1 6$	(4)	1.625	1.623	1.622(1)	1.624(1)
$O_1 6$-$T_1 6$-$O_1 6'$	(2)	119.23	118.37	118.63(5)	119.18(4)
-$O_1 6'''$	(2)	110.98	111.20	110.78(6)	110.87(4)
-$O_1 6'$	(2)	98.84	99.39	99.56(5)	98.99(3)
Mean		109.68	109.65	109.66	109.67
$T_2 1$-$O_1 1$	(2)	1.631	1.631	1.631(1)	1.630(1)
-$O_2 3'$	(1)	1.607	1.609	1.606(2)	1.608(1)
-$O_2 1$	(1)	1.582	1.588	1.589(2)	1.588(1)
Mean		1.6128	1.6148	1.6143	1.6148
$O_1 1$-$T_2 1$-$O_1 1m$	(1)	107.84	108.40	108.26(6)	108.12(4)
-$O_2 1$	(2)	109.85	110.15	109.98(6)	109.93(4)
-$O_2 3'$	(2)	108.45	108.80	108.50(5)	108.46(4)
$O_2 1$-$T_2 1$-$O_2 3'$	(1)	112.27	110.49	111.54(9)	111.85(6)
Mean		109.45	109.47	109.46	109.46
$T_2 3$-$O_1 3$	(2)	1.632	1.628	1.627(1)	1.632(1)
-$O_2 3$	(1)	1.614	1,616	1.615(2)	1.612(1)
-$O_2 6$	(1)	1.578	1.585	1.582(2)	1.579(1)
Mean		1.6140	1.6143	1.6128	1.6138
$O_1 3$-$T_2 3$-$O_1 3m$	(1)	108.37	109.00	108.68(7)	108.54(5)
-$O_2 6$	(2)	111.65	111.72	111.95(5)	111.74(4)
$O_2 3$	(2)	107.19	107.64	107.29(5)	107.23(4)
$O_2 6$-$T_2 3$-$O_2 3$	(1)	110.59	108.95	109.47(9)	110.17(7)
Mean		109.44	109.45	109.44	109.44
$T_2 6$-$O_1 6$	(2)	1.768	1.762	1.762(1)	1.766(1)
-$O_2 1$	(1)	1.711	1.713	1.713(2)	1.710(1)
-$O_2 6$	(1)	1.713	1.719	1.717(2)	1.714(1)
Mean		1.7400	1.7390	1.7385	1.7390
$O_1 6$-$T_2 6$-$O_1 6m$	(1)	105.74	105.88	106.55(5)	105.91(5)
-$O_2 6$	(2)	108.28	108.90	108.76(5)	108.48(4)
-$O_2 1$	(2)	110.43	111.25	110.96(5)	110.66(4)
$O_2 1$-$T_2 6$-$O_2 6$	(1)	113.36	110.54	110.73(8)	112.40(1)
Mean		109.42	109.45	109.45	109.43
$T_2 1$-$O_2 1$-$T_2 6$	(2)	173.81	170.3	172.3(1)	172.96(12)
$T_2 1$-$O_2 3$-$T_2 3$	(2)	179.78	178.6	179.3(1)	179.68(10)
$T_2 3$-$O_2 6$-$T_2 6$	(2)	162.44	161.0	160.1(1)	161.78(8)
Mean		172.01	170.0	170.6	171.47

Table 5—*Continued*

dist./angl.	mult.	Sponda	Kemiö	Ferry	Haddam
$T_2$1-$O_1$1-$T_1$1	(2)	127.94	129.08	128.25(7)	128.11(5)
$T_2$6-$O_1$6-$T_1$6	(2)	132.84	132.99	133.45(7)	132.96(5)
$T_2$3-$O_1$3-$T_1$1	(2)	128.45	128.79	128.85(7)	128.42(5)
Mean		129.7	130.29	138.18	129.83
$T_1$1-$O_1$1-M	(2)	95.01	95.09	94.78(5)	94.93(4)
$T_1$1-$O_1$3-M	(2)	94.22	93.83	93.72(6)	94.13(4)
$T_1$6-$O_1$6-M	(2)	95.16	95.31	94.61(5)	95.10(4)
$T_2$1-$O_1$1-M	(2)	136.91	135.63	136.77(7)	136.80(5)
$T_2$3-$O_1$3-M	(2)	137.01	136.87	137.00(7)	137.08(5)
$T_2$6-$O_1$6-M	(2)	131.59	131.22	131.32(7)	131.52(4)
Mean		114.98	114.66	114.70	114.93
M -$O_1$6	(2)	2.129	2.158	2.133(1)	2.133(1)
-$O_1$1'	(2)	2.104	2.112	2.120(1)	2.105(1)
-$O_1$3'	(2)	2.128	2.146	2.148(1)	2.132(1)
Mean		2.1203	2.1387	2.1337	2.1233
Na-Ch1/4	(2)	2.3304	2.3232	2.3337(5)	2.3309(5)
Na-$O_2$6	(2)	2.513	2.499	2.481(2)	2.501(1)
Na-$O_2$3	(2)	2.893	2.876	2.879(2)	2.891(1)
Na-$O_2$1	(2)	2.717	2.666	2.699(2)	2.705(1)
Mean		2.6134	2.5911	2.5989	2.6080

the Ferry cordierite does not bear substantial Be is confirmed by the relatively long, corrected mean $T_1$1–O bond, which ranks this value with those of the Be-poor cordierites of Wallace and Wenk (1980) in Figure 2. Refined fractional coordinates as listed in Table 4 reveal that the largest changes involve $O_2$6 and $O_2$1 in the various structures. The bond lengths (Table 5) indicate that the $O_2$1–Na and $O_2$6–Na bonds are most affected by this variation. With increasing Na occupation on Ch0, the $O_2$1–Na distance decreases and also $O_2$6–Na and $O_2$3–Na decrease slightly (Fig. 3). Including the Wallace and Wenk (1980) data, linear regression analyses ($N = 10$) yielded

$$O_2\text{1–Na} = 2.755(2) - 0.176(9)\cdot OC(Na), \quad R = -99.0\%, \tag{1a}$$

$$O_2\text{6–Na} = 2.528(4) - 0.089(15)\cdot OC(Na), \quad R = -89.4\%, \tag{1b}$$

$$O_2\text{3–Na} = 2.911(2) - 0.076(8)\cdot OC(Na), \quad R = -96.3\%, \tag{1c}$$

where OC is the atomic occupation of Na in Ch0.

All cordierites studied in this paper have (within 3σ) the same mean bond lengths (Table 5) between oxygen and the tetrahedrally coordinated positions $T_2$1 and $T_2$3 ($T_2$1–O, $T_2$3–O = 1.614 Å) indicating uniform Si occupation at these ring positions. There is also no significant difference (greater than 3σ) between the mean bond lengths within the AlO_4 tetrahedra around $T_2$6 ($T_2$6–O = 1.739 Å) and within the SiO_4 tetrahedra around $T_1$6 ($T_1$6–O = 1.623 Å) interconnecting the rings, which demonstrates a well-ordered arrangement of (Si,Al) in these cordierites. Cohen et al. (1977) showed conclusively that the size difference between the Si tetrahedra $T_2$1 and $T_2$3 on the one hand and $T_1$6 on the other is strongly dependent upon the angular distortion (T–O–T) and should not be used to postulate differences in the (Si,Al) content.

In order to get a proper evaluation of the dependence of structural distortions upon Na content, two samples that are structurally similar except for their Na content in Ch0 were compared. Be-bearing crystals are not appropriate for this purpose because the variable size of the

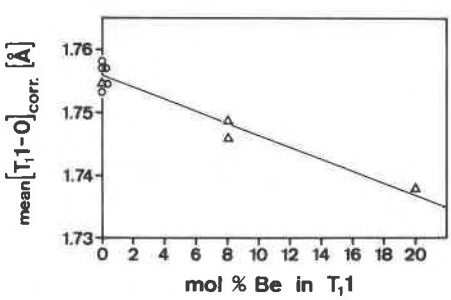

Fig. 2. Correlation between Be substitution in $T_1$1 and the mean, *F*-corrected $T_1$1–O bond length. The size of the symbols describes one standard deviation (σ) of the observed bonds [triangles: this paper; circles: Wallace and Wenk (1980)]. The solid line connects the mean value (1.756 Å) observed for Be-free cordierites with a bond length of 1.66 Å, as obtained for beryls where the corresponding position is fully occupied by Be.

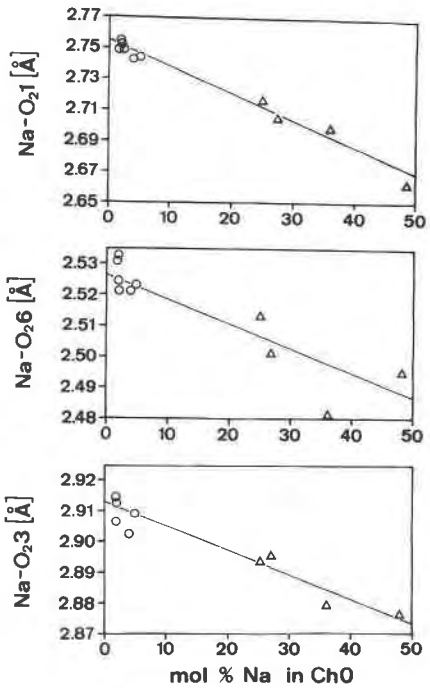

Fig. 3. Dependence of Na–O distances on Na occupation in the center of the six-membered rings. The size of the symbols describes two standard deviations (σ) of the Na–O bond lengths [triangles: this paper; circles: Wallace and Wenk (1980)]. Solid lines result from linear regression analyses (Eqs. 1a–1c).

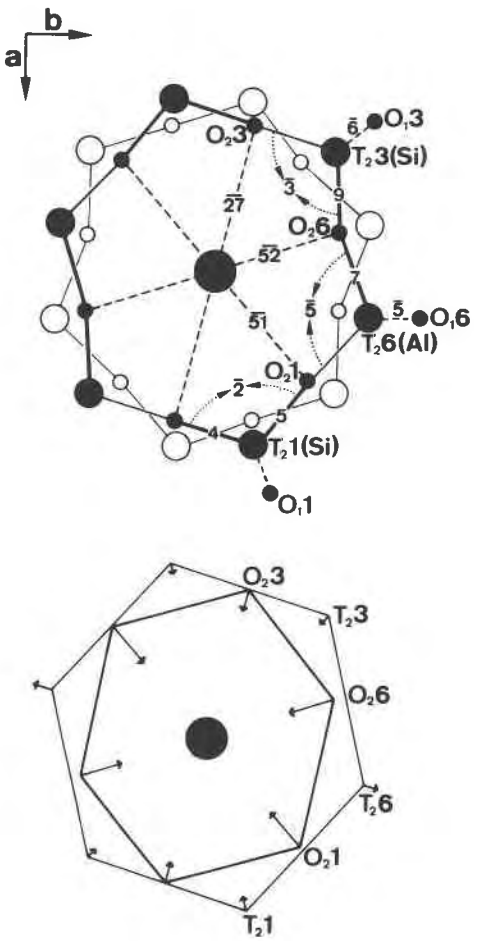

Fig. 4. Distortion of the six-membered rings of tetrahedra owing to Na incorporation. The figure is based on a comparison between the crystal structures of the Na-poor specimen Sci552 (Wallace and Wenk, 1980) and the Na-rich Ferry crystal.

Upper figure: A ring at $z = 0$ is emphasized by connection of filled circles centered by Na at Ch0 (site symmetry 222). Open circles indicate atom positions at $z = \pm 1/2$. Decrease of Ch0–O distances owing to Na in Ch0 is indicated by dashed lines. The amount of change is given in 0.001 Å. Heavy solid lines specify increased anion-cation distances. Decrease of T–O–T angles is shown by dotted curves given for each angle. The change of angles is in full degrees.

Lower figure: Oxygen atoms at $z = 0$ are connected with each other to form an inner ring. Also shown are cations at $z = 0$ to form an outer ring. Arrows indicate the relative motion due to Na incorporation. The oxygen ring contracts mainly along the vector Na–$T_2$6, whereas the cation ring expands along this direction.

$T_1$1 tetrahedron (due to Be → Al substitution) introduces additional distortion.

One appropriate sample is the Ferry cordierite that is Na rich but essentially Be free and exhibits a mean M–O distance of 2.133 Å. The second appropriate specimen is the (Mg,Fe)-cordierite "Sci552" of Wallace and Wenk (1980) that is Na poor with a mean M–O distance of 2.134 Å. To investigate the effect of Na, interatomic distances and angles are compared using Ch0 as a reference point. Figure 4 elucidates what is happening when Na occupies the Ch0 site.

The dominant influence of Na is a decrease in the bottleneck diameter (at $z = 0$) caused by the attraction of ring oxygen atoms for Na. This interaction is especially strong for $O_2$1 and $O_2$6 which, linking a Si with an Al tetrahedron, may carry a locally unbalanced negative charge. These oxygen atoms also form the shortest T–O bonds in the ring tetrahedra. Consequently, the tetrahedron around $T_2$6, where Al is bonded to $O_2$1 and $O_2$6, shows the greatest variation with Na content. An adjustment of 5° in the tetrahedral angle $O_2$6–$T_2$6–$O_2$1 of the Ferry cordierite pushes $T_2$6 outward. This mechanism is additionally enhanced by a slight increase of the $T_2$6–$O_2$6 bond length. The resulting distortion is comparable to an O–T–O scissoring motion combined with a translation of $T_2$6.

The oxygen atoms ($O_2$1, $O_2$3, $O_2$6) forming corners of the tetrahedra $T_2$1 and $T_2$3 are differently attracted by Na, which slightly tilts the tetrahedra. The lesser flexibility of the Si tetrahedra in terms of O–T–O angles which decrease only 2–3° is thus responsible for the movement of the Si atoms in $T_2$1 and $T_2$3 toward the channel center. Neither the slight variation in the tetrahedral angle nor the minute expansion of the $T_2$1–$O_2$3, $T_2$1–$O_2$1, and $T_2$3–$O_2$6 bonds is sufficient to "buffer" the oxygen attraction for Na.

As mentioned above, all Na-rich cordierites studied reveal only insignificant differences in the mean T_2(Si)–O

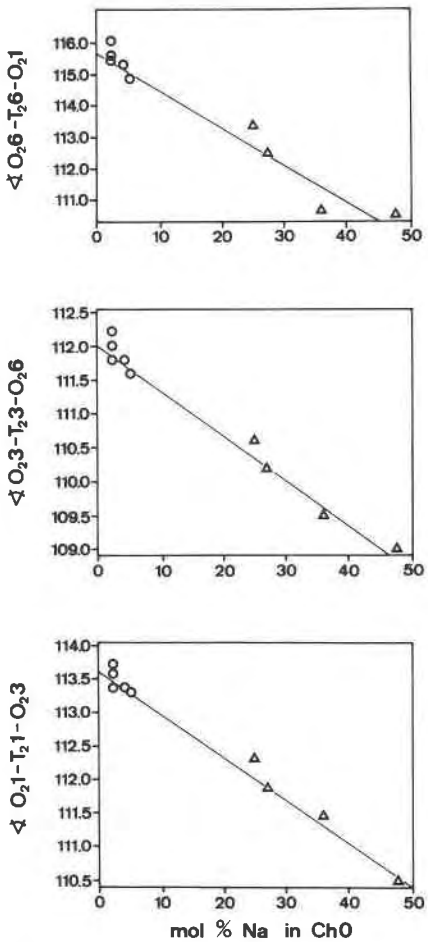

Fig. 5. Dependence of O–T–O angles on Na concentration in Ch0 [circles: Wallace and Wenk (1980); triangles: this paper]. The size of the symbols specifies about one standard deviation (σ) of the measured angle. Solid lines result from linear regression analyses (Eqs. 2a–2c).

and T_2(Al)–O distances, which seems to contradict the observed expansion of individual T_2–O_2 bonds. However, the T_2–O_1 bonds, which occur twice per tetrahedron (mirror related), contract modestly and decrease the mean T_2–O distance. As can be seen in Figure 4, Na in Ch0 causes the individual six-membered oxygen rings to compress along the vector T_26–Na, while T_26 is pushed outward owing to the scissoring motion. This opposite motion is responsible for the decrease in the lattice distortion index [$\Delta = 1.094 \cdot (a - b\sqrt{3})$] with increasing Na content, a correlation frequently emphasized by mineralogists for (Si,Al) ordered, hydrous cordierites (Schreyer et al., 1979; Selkregg and Bloss, 1980; Armbruster and Irouschek, 1983).

It must be kept in mind that the effect of Na on the structure of cordierite has only been established for Be-free crystals, which are rare in nature. This raises the question of whether or not the described deformation can be extended to hydrous Na-rich cordierites in general. Therefore, a set of linear regression analyses with Na content as the independent variable has been carried out by combining the bond lengths and angles of Na-poor cordierites (Wallace and Wenk, 1980) with those from Na-rich crystals ($N = 10$). The results indicate an excellent inverse correlation (Fig. 5) between Na and the tetrahedral angles formed between T_2(Si,Al) and two ring oxygen atoms.

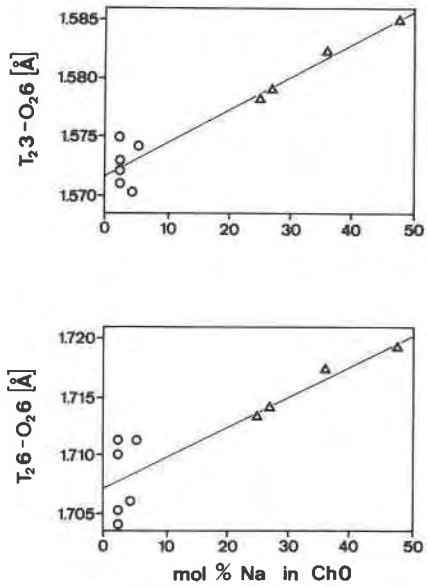

Fig. 6. Dependence of T–O distances on Na concentration in Ch0 [circles: Wallace and Wenk (1980); triangles: this paper]. The size of the symbols indicates about one standard deviation (σ) of the bond length. Solid lines result from linear regression analyses (Eqs. 3a, 3b).

$$O_26\text{–}T_26\text{–}O_21 = 115.8(2) - 11.8(9)\cdot OC(Na), \quad R = -97.92\%, \tag{2a}$$

$$O_23\text{–}T_23\text{–}O_26 = 112.07(7) - 6.3(3)\cdot OC(Na), \quad R = -99.16\%, \tag{2b}$$

$$O_21\text{–}T_21\text{–}O_23 = 113.66(6) - 6.3(3)\cdot OC(Na), \quad R = -99.30\%. \tag{2c}$$

Oxygen atoms that move the most toward the channel center (O_26 and O_21) also cause the largest decrease of the tetrahedral angle. It is obvious that corresponding correlations can be found between Na and the T–O–T angles in the six-membered ring. The influence of Na on the tetrahedral bond lengths (Fig. 6), however, is not as pronounced. Only T_26–O_26 and T_23–O_26 have a high correlation between lengthening and increasing Na content.

$$T_26\text{–}O_26 = 1.707(1) + 0.026(5)\cdot OC(Na), \quad R = 88.31\%, \tag{3a}$$

$$T_23\text{–}O_26 = 1.5717(7) + 0.028(3)\cdot OC(Na), \quad R = 95.61\%. \tag{3b}$$

It must be assumed that cooperative effects and other minor substitutions occurring in natural cordierites also influence the tetrahedral bonds (e.g., Wallace and Wenk, 1980).

The following pattern emerges from Figure 4 and Equa-

tions 2a–3b. In Na-poor cordierites, Al tetrahedra are more distorted in their O–T–O angles than corresponding Si tetrahedra ($T_1$1 vs. $T_1$6 and $T_2$6 vs. $T_2$1, $T_2$3). With increasing Na content, the ring tetrahedra become more regular in their angles. This effect, which is strongest in the tetrahedron around $T_2$6, allows $O_2$1 and $O_2$6 to approach Na without Al moving toward Na. The Be-bearing tetrahedron $T_1$1 is corner-linked to the tetrahedra around $T_2$1 and $T_2$3. In case of Na + Be → Al substitution, both the smaller size of $T_1$1 and the shift of $T_2$1 and $T_2$3 toward Na (Fig. 3) yield a shortening in the lattice mainly along the vector ⟨110⟩, which has a greater effect on *a* than on *b*.

It should be noted that all distortions interpreted as being due to Na are actually caused by Na and two type II water molecules positioned above and below Na in the adjacent cavities. The differences between the influence of Na in anhydrous and hydrous cordierites has been discussed (Armbruster, 1985a). In anhydrous cordierites, Na is not fixed at Ch0 but shows increased thermal motion along the channel axis, which also weakens its influence on the bottleneck-forming tetrahedra.

Temperature factors

The oxygen atoms ($O_2$6, $O_2$1, and $O_2$3) common to tetrahedra in the six-membered ring vibrate most strongly parallel to the c-axis. Within (001), the vibration is directed toward the channel center. In previous papers (Cohen et al., 1977; Hochella et al., 1979), O_2 positions with high isotropic temperature factors and O_1 positions with lower ones were classified in two groups, two-coordinated oxygens (O_2) and three-coordinated oxygens (O_1). This distinction cannot be made in Na-rich crystals, because, strictly speaking, the ring oxygens are coordinated to Na in Ch0 and are thus three-coordinated. Dependence of the O_2 temperature factors with varying Na occupation in the ring center is statistically significant only for $O_2$1. With increasing Na content, the squared vibrational amplitude (U) of $O_2$1 along the vector $O_2$1–Ch0 increases:

$$U_{O_21} = 0.0139(5) + 0.0127(24)\cdot \mathrm{OC(Na)},\ R = 88.1\%. \quad (4)$$

This is surprising because an inverse correlation would be expected, namely a decrease of thermal vibration when Na is introduced into the ring center. The observed behavior can be explained by a disorder model: within a Na-rich cordierite crystal, certain six-membered rings, randomly distributed over the structure, are centered by Na and show short $O_2$1–Ch0 distances (as shown by Eq. 1a), whereas the remaining $O_2$1–Ch0 distances in empty rings are longer. The observed $O_2$1–Ch0 bond length is therefore a mean distance between the two positions and the increase of U_{O_21} along the bond direction reflects static disorder. This effect is especially strong for the temperature factor $O_2$1 because the influence of Na occupancy is also the strongest on the $O_2$1–Ch0 bond. For $O_2$3–Ch0 and $O_2$6–Ch0, the decrease in distance with increasing Na is considerably smaller and also not as well correlated.

Chandrasekhar and Bürgi (1984) have recently shown that information about dynamic or static disorder is provided by difference vibrational parameters (ΔU), evaluated between bonded atoms. However, the ΔU approach does not yield information in this case because of the high correlation between occupational and vibrational parameters. For example, small errors in the amount of Na in Ch0 would cause a substantial effect on the value of U_{Na}.

The highest temperature factors, probably related to static as well as dynamic disorder, are found for the channel positions Ch0 and Ch¼. Na has its largest thermal parameter parallel to the structural channel, while the oxygen atom assigned to Ch¼ has its largest temperature factor parallel to the **a** axis, reflecting the shape of the oblate structural cavity around Ch¼. In general, Si and/or Al temperature factors for identical positions within different crystals are only in fair agreement, particularly for U_{33}. It is unclear whether these discrepancies are caused by differences in the chemical composition giving rise to structural distortions, or by some systematic effects such as anisotropic extinction. Inspection of the structure-factor tables (Table 3) indicates that F_{calc} of the crystals with the highest isotropic extinction parameter are still too high compared to F_{obs} for reflections of the type 00*l*. This systematic error could increase temperature factors parallel to **c**.

As shown by Chandrasekhar and Bürgi (1984), the substantial size difference between Be (Be–O = 1.66 Å) and Al (Al–O = 1.76 Å) in the $T_1$1 tetrahedron should cause an increase of the difference vibrational parameter ΔU related to static disorder. This relation is apparent, but a larger data base and correction for cooperative effects such as increase of $T_1$1 owing to Fe → Mg substitution is necessary for detailed examination.

As already mentioned, minor substitution of Li^+ for Mg^{2+} or Fe^{2+} in the M site will not have a strong effect on the mean M–O bond length. However, the refined temperature factors for this position are highly sensitive to the degree of Fe-Mn-Mg-Li substitution. If too strong a scattering is presumed at M, e.g., due to overestimation of the amount of Fe, the refined temperature factor will compensate for this by refining to a larger value. The observed temperature factors for M still show strong variations between various structures that might be related to the difficulty in determining the true occupation of the M site. Previous work (Armbruster and Schenk, 1984) disclosed that about 10 mol% of the total Fe is Fe^{3+}. It is not known whether the ferric component resides in the octahedron (M), tetrahedron, or channel position or in several sites. This lack of knowledge introduces errors in estimating the Li content from the difference between the theoretical value of 2 and the observed moles of Mg + Fe + Mn calculated on the basis of 18 oxygen atoms.

Channel occupants in Ch¼

Difference-Fourier maps (Fig. 7) were obtained from structure-factor calculations with channel constituents removed from sites Ch0 and Ch¼. The oxygen of the water molecule in Ch¼ exhibits an almost circular electron dis-

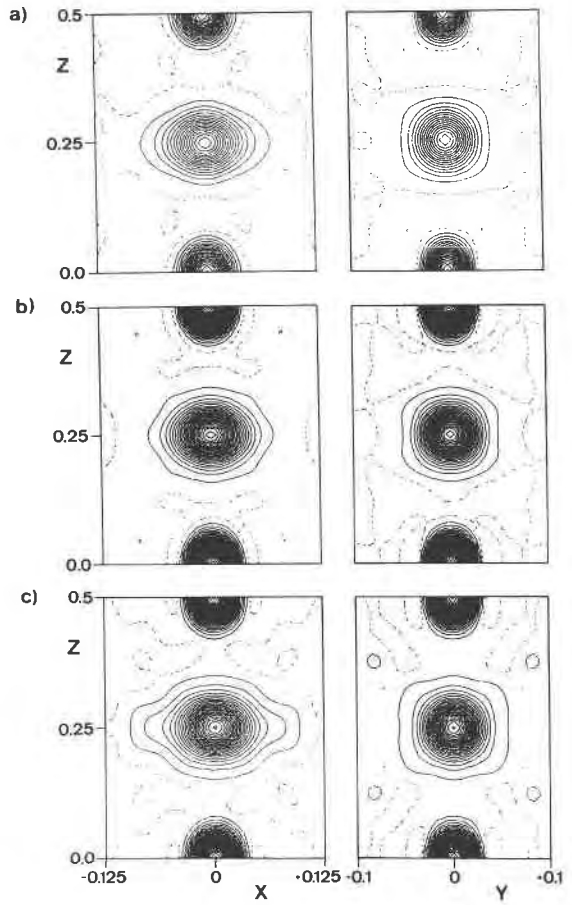

Fig. 7. Difference-Fourier maps calculated with removed channel occupants at Ch0 and Ch¼. All sections are through the center of the cavity. Negative contours are omitted, dashed contours indicate 0 e/Å³, solid contours are positive with an interval of 0.5 e/Å³. The following maximum electron densities were observed within the structural channels: (a) Sponda cordierite—at Ch0, 5.2 e/Å³; at Ch¼, 6.0 e/Å³. (b) Kemiö cordierite—at Ch0, 11.0 e/Å³; at Ch¼, 7.5 e/Å³. (c) Ferry cordierite—at Ch0, 9.5 e/Å³; at Ch¼, 7.4 e/Å³.

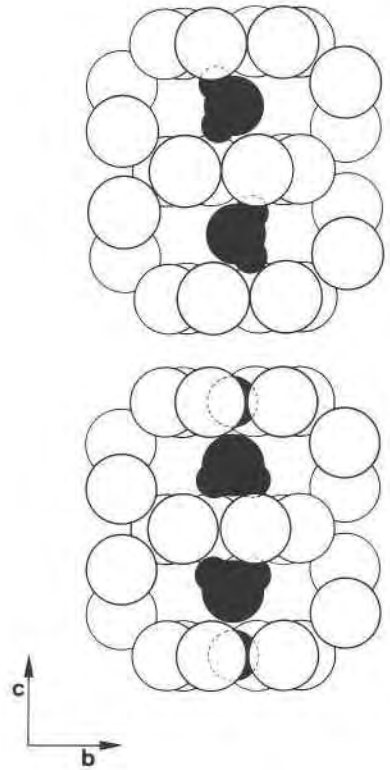

Fig. 8. A portion of the cordierite structure, viewed down the **a** axis, showing only those oxygen atoms that form a single channel in the cordierite framework. Three bottlenecks are thus viewed edgewise, and midway between the centers of each two bottlenecks are the open cages. The upper drawing shows the possible disorder of the water molecule type I, and the lower drawing, the water molecule type II. Both types coexist in the cordierites studied.

tribution in the (100) sections. In (010) projections, the density becomes elongated parallel to **a**, particularly in the Ferry cordierite. Wallace and Wenk (1980) displaced the water molecule from the center of the cavity (222 symmetry) and unsuccessfully tried to refine "split water positions." Finally they interpreted these asymmetric bulges of the H_2O density as a result of hydrogen polarization associated with a split water molecule with an oxygen position closer to the ring oxygen atoms $O_2$1 and $O_2$6. This split water position was also described by Hochella et al. (1979) for the natural White Well cordierite but again could not be refined. On the basis of neutron and X-ray $\Delta\rho$ maps, the latter authors postulated a new water orientation with the plane of the molecule inclined by 29° from (100) and the H-H vector 19° from **c** and rejected the hypothesis that the observed density is caused by the presence of both water types (types I and II). X-ray structure work on a degassed White Well cordierite, partially filled with CO_2 under elevated temperature and pressure conditions (Armbruster and Bürgi, 1982), disclosed that CO_2 is aligned with its O–C–O vector mainly parallel to the **a** axis, yielding additional peaks at 0.017,0,¼ in difference-Fourier maps. In the natural White Well cordierite, used by Hochella et al. (1979) for their structural study, 33% of the cavities are filled by water and an additional 8% by CO_2 (Armbruster and Bloss, 1982). It remains questionable whether the presence of CO_2, which was not known at this time, led to an overinterpretation of the $\Delta\rho$ maps. Thus the H_2O orientation of Hochella et al. (1979) may be erratic. Unfortunately, no precise CO_2 analyses are available for the samples of Wallace and Wenk. Our own optical studies on the crystals Sci1542 and Sci1018, picked from the same thin section from which the crystals of the structure work originated, revealed relatively high optic angles ($2V_X$) of 86° and 80°, respectively, and a birefringence of 0.012 (n_α = 1.5440, n_γ = 1.5560) for Sci1018. These results rank these specimens as fairly CO_2-rich (Armbruster and Bloss, 1982) with a total gas content (H_2O + CO_2) of 2.7 wt% for Sci1018 as calculated from

the refractive indices and F value (Lepezin et al., 1976). On the basis of these findings, the smeared-out electron density parallel to the **a** axis (Fig. 7) can be explained by the presence of CO_2 in the structural cavity, and models postulating split water positions or other "complicated" water orientations need not be invoked.

Assuming that each Na in Ch0 is coordinated by two water molecules of type II in Ch¼ at $z = ¼$ and $z = -¼$, then all crystals studied in this paper predominantly possess water of type II (Fig. 8) and only minor amounts of water of type I. This was confirmed by IR powder spectra of the Sponda, Ferry, and Haddam samples, which in addition displayed a weak 3689 cm^{-1} absorption characteristic of water of type I. Furthermore, the latter samples contain CO_2-occupied cages in various amounts: Haddam, 2%; Sponda, 4%; and Ferry, <10%. No data are available for the Kemiö sample, but the shape of the electron cloud around Ch¼ does not much differ from the other crystals. Difference-Fourier maps with included channel positions for the Ferry crystal display residual peaks (0.5 e/Å^3) at positions similar to the ones observed for oxygen atoms of CO_2 (Armbruster and Bürgi, 1982). The residual density for the other room-temperature refinements around Ch¼ is about 0.3 e/Å^3 and generally smeared out along **a**.

Acknowledgments

J. M. Ferry (Baltimore) and P. Povondra (Praha) kindly supplied portions of their samples for this investigation. G. Werding (Bochum) provided Li analyses, which were highly appreciated. An earlier version of this manuscript benefited from the constructive reviews of G. A. Lager (Louisville) and R. Kirchner (New York).

References

Armbruster, Th. (1985a) Effect of H_2O on the structure of low cordierite: A single crystal X-ray study. Proceedings of the IMA Meeting 1982, Varna, Bulgaria (in press).

——— (1985b) Fe-rich cordierites from acid volcanic rocks, an optical and X-ray single-crystal structure study. Contributions to Mineralogy and Petrology, 91, 180–187.

Armbruster, Th., and Bloss, F.D. (1982) Orientation and effects of channel H_2O and CO_2 in cordierite. American Mineralogist, 67, 284–291.

Armbruster, Th., and Bürgi, H.B. (1982) Orientation of CO_2 in the cavity of cordierite, a single crystal X-ray study at 100, 300 and 500 K. Fortschritte der Mineralogie, 60, Beiheft 1, 37–39.

Armbruster, Th., and Irouschek, A. (1983) Cordierites from the Lepontine Alps: Na + Be → Al. Substitution, gas content, cell parameters and optics. Contributions to Mineralogy and Petrology, 82, 389–396.

Armbruster, Th., and Schenk, K. (1984) Crystal structure, optical properties, and chemistry of cordierites from acid volcanic rocks. Fortschritte der Mineralogie, 62, Beiheft 1, 10–12.

Bloss, F.D. (1981) The spindle stage, principles and practice. Cambridge University Press, Cambridge.

Carson, D.G., Rossman, G.R., and Vaughan, R.W. (1982) Orientation and motion of water molecules in cordierites: A proton nuclear magnetic resonance study. Physics and Chemistry of Minerals, 8, 14–19.

Černý, P., and Povondra, P. (1966) Beryllian cordierite from Věžná: (Na,K) + Be → Al. Neues Jahrbuch für Mineralogie Monatshefte, 44, 36–44.

Chandrasekhar, K., and Bürgi, H.B. (1984) Dynamic processes in crystals examined through difference vibrational parameters ΔU: The low-spin–high-spin transition in Tris(dithiocarbamato)iron(III) complexes. Acta Crystallographica, B40, 387–397.

Cohen, J.P., Ross, F.K., and Gibbs, G.V. (1977) An X-ray and neutron diffraction study of hydrous low cordierite. American Mineralogist, 62, 67–78.

Enraf Nonius. (1983) Structure determination package (SDP). Enraf Nonius, Delft.

Ferry, J.M. (1980) A comparative study of geothermometers and geobarometers in pelitic schists from south-central Maine. American Mineralogist, 65, 720–732.

Fuchs, L.H. (1969) Occurrence of cordierite and aluminous orthoenstatite in the Allende meteorite. American Mineralogist, 54, 1645–1653.

Gibbs, G.V. (1966) The polymorphism of cordierite I: The crystal structure of low cordierite. American Mineralogist, 51, 1068–1081.

Gibbs, G.V., Breck, D.W., and Meagher, E.P. (1968) Structural refinement of hydrous and anhydrous synthetic beryl, $Al_2(Be_3Si_6)O_{18}$ and emerald, $Al_{1.9}Cr_{0.1}(Be_3Si_6)O_{18}$. Lithos, 1, 275–285.

Goldman, D.S., Rossman, G.R., and Dollase, W.A. (1977) Channel constituents in cordierite. American Mineralogist, 62, 1144–1157.

Hochella, M.F., Brown, E.B., Ross, F.K., and Gibbs, G.V. (1979) High-temperature crystal chemistry of hydrous Mg- and Fe-cordierites. American Mineralogist, 64, 337–351.

Lepezin, G.G., Lavrent'ev, Yu.G., and Pokachalova, O.S. (1974) Problems of alkalies in cordierites (in Russian). Geologia i Geophisica Akademia Nauk SSSR, Sibirskoye Otdeleniye, 3, 93–96.

Lepezin, G.G., Kuznetsova, I.K., Lavrent'ev, Yu.G., and Cheml'nicova, O.S. (1976) Optical methods of determination of water contents in cordierite. Contributions to Mineralogy and Petrology, 58, 319–329.

Meagher, E.P. (1967) The crystal structure and polymorphism of cordierite. Ph.D. thesis, Pennsylvania State University, University Park.

Morosin, B. (1972) Structure and thermal expansion of beryl. Acta Crystallographica, B28, 1899–1903.

Newton, R.C. (1966) BeO in pegmatitic cordierite. Mineralogical Magazine, 35, 920–927.

Povondra, P., and Čech, F. (1978) Sodium-beryllium-bearing cordierite from Haddam, Connecticut, USA. Neues Jahrbuch für Mineralogie Monatshefte, 1978, 203–209.

Povondra, P., Čech, F., and Burke, E.A.J. (1984) Sodian-beryllian cordierite from Gammelmorskärr, Kemiö Island, Finland, and its decomposition products. Neues Jahrbuch für Mineralogie Monatshefte, 1984, 125–136.

Povondra, P., and Langer, K. (1971) Synthesis and some properties of sodium-beryllium bearing cordierite $Na_xMg_2(Al_{4-x}Be_xSi_5O_{18}$. Neues Jahrbuch für Mineralogie Abhandlungen, 116, 1–19.

Schreyer, W., Gordillo, C.E., and Werding, G. (1979) A new sodian-beryllian cordierite from Soto, Argentina, and the relationship between distortion index, Be-content, and state of hydration. Contributions to Mineralogy and Petrology, 70, 421–428.

Selkregg, K.R., and Bloss, F.D. (1980) Cordierites: Compositional controls of Δ, cell parameters, and optical properties. American Mineralogist, 65, 522–533.

Shannon, R.D. (1976) Revised effective ionic radii and systematic studies of interatomic distances in halides and chalcogenides. Acta Crystallographica, A32, 751–767.

Stewart, J.M., Machin, P.A., Dickinson, C.W., Ammon, H.L., Heck, H., and Flack, H. (1976): The X-ray system of crystallographic programs, version of 1976. University of Maryland Computer Science Center Technical Report TR-445, College Park, Maryland.

Wallace, J.H., and Wenk, H.R. (1980) Structure variation in low cordierites. American Mineralogist, 65, 96–111.

Manuscript received May 2, 1985
Manuscript accepted January 17, 1986